

# Sustainable Arctic observing network for forecasting weather extremes over the mid-latitudes



Jun Inoue<sup>1,2</sup>, Kazutoshi Sato<sup>1</sup>, and Akira Yamazaki<sup>2</sup>

(1: National Institute of Polar Research, Japan, 2: JAMSTEC, Japan)



## 1. Introduction

Recent cold winter extremes over Eurasia and North America have been considered to be a consequence of a warming Arctic. More accurate weather forecasts are required to reduce human and socioeconomic damages associated with severe winters. However, the sparse observing network over the Arctic brings errors in initializing a weather prediction model, which might impact accuracy of prediction results at midlatitudes.

During February 2015, the jet stream frequently meandered over East Asia and eastern North America, causing anomalous low temperatures in these regions (Fig. 1). During the same period, increased radiosonde observations were made on a ship drifting in Arctic sea ice and at several existing operational stations (Fig. 2a). In the present study, we present the impacts of these additional radiosonde observation data over the Arctic region for forecasting of the Cold Air Outbreaks (CAOs) in February 2015 over midlatitudes, using an ensemble data assimilation system and observing system experiments.

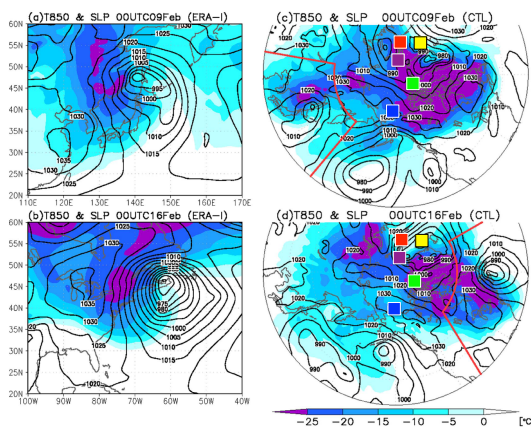


Figure 1: Temperature at 850 hPa (shaded: °C) and sea level pressure (contour: hPa) over (a) East Asia at 0000 UTC 9 February, and (b) eastern North America at 0000 UTC 16 February 2015 in ERA-Interim. The same information in Figures 1c and 1d but for ALERA2 (CTL) reanalysis. Areas enclosed by red line correspond to the areas in Figures 1a and 1b. Squares indicate radiosonde stations shown in Figure 2a.

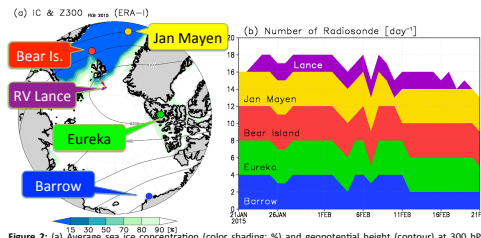


Figure 2: (a) Average sea ice concentration (color shading: %) and geopotential height (contour: hPa) at 300 hPa (Z300) during February 2015 in ERA-Interim. Color dots indicate radiosonde stations (blue: Barrow, green: Eureka, red: Bear Island, Jan Mayen). Track and radiosonde observation points of RV Lance during Floe 1 of N-ICE 2015 are shown by orange line and purple dots. (b) Number of daily radiosondes at the stations.

## 2. Radiosonde Observations

- RV Lance during Norwegian young sea ICE expedition (N-ICE2015) twice daily at 0000 and 1200 UTC
- Existing stations at **Bear Island, Jan Mayen, Eureka, and Barrow** twice daily (regular: 0000 & 1200 UTC) + two additional launches (0600 & 1800 UTC)
- The sent data to the Global Telecommunication System (GTS) were presumed to improve reanalysis products and operational weather forecasts. (Fig. 2b)

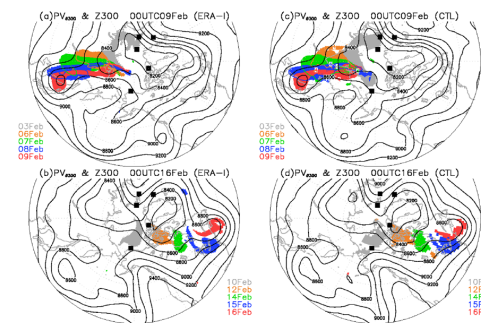


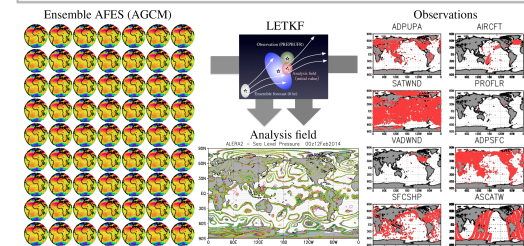
Figure 3: Potential vorticity >4 PVU on 300 K surface at 0000 UTC on each day (color shading: PVU), and geopotential height (contours at 300 hPa level (Z300): m) at 0000 UTC 09 February (top) and 0000 UTC 16 February (bottom). Some PV fields are masked to highlight temporal evolution of targeted PV. Data are based on (a, b) ERA-Interim reanalysis and (c, d) ALERA2 (control reanalysis: CTL). Contours indicate averaged Z300 (m) during forecast periods.

Table 1: Model description.

Resolution	T119L48 (~1°×1°, up to ~3 hPa)
Ensemble size	63+1
Covariance localization	$\sigma=400 \text{ km} / 0.4 \text{ ln}p$
Spread inflation	10% (fixed)
Observations	NCEP PREPBUFR
Boundary conditions	OISST daily 1/4°
DA window	6 h

## 3. Ensemble Reanalysis and Forecasts

- Data assimilation system **ALEDAS2** (Table 1)  
Atmospheric general circulation model for the Earth Simulator (**AFES**)  
+ Local ensemble transform Kalman filter (**LETKF**).
- Two sets of experimental ensemble reanalysis **ALERA2**  
**CTL**: including all NCEP PREPBUFR data sets  
**OSE**: excluding all additional radiosonde station data
- Reproducibility  
CTL well reproduced the atmospheric field comparing with ERA-Interim (Fig. 3)  
**OSEF**: initialized by OSE
- Two sets of ensemble forecasts (5 days forecast with 63 members)  
**CTLf**: initialized by CTL  
**OSEF**: initialized by OSE
- Target cases  
East Asian cold event: 9 February 2015  
North US cold event: 16 February 2015



## Eastern Asia event

- 4. Extreme cold events during February 2015
- Western high & eastern low pressure pattern; Cold air masses over continents
- Cold core corresponded to southward intrusion of upper high-PV; tropopause fold

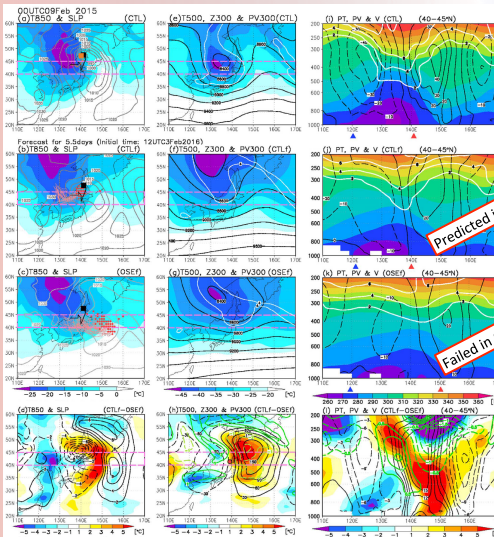


Figure 4: 1850 (color shading: °C) and SLP (contours: hPa) at 0000 UTC 9 February 2015 in (a) CTL, (b) CTLf, and (c) OSEF. Difference between CTLf and OSEF is shown in Figure 4d. (e-f) Same as Figures 4a-d, but for 1500 (color shading: °C), Z300 (contours), and PV at 300 hPa (white lines: 4 PVU). Longitude-height cross sections of PV (color shading: K), meridional winds (black contours: m s<sup>-1</sup>), and PV (white contours: PVU) averaged over areas between 40°N and 45°N (pink lines) shown in Figures 4i-k; the difference between (j) and (k) is also shown in Figure 4l. Black and orange lines in Figure 4a show track of a cyclone from 1800 UTC 7 February through 0000 UTC 9 February in CTL and ERA-Interim. Red lines in Figures 4b and 4c show track of a cyclone from 1800 UTC 7 February through 0000 UTC 9 February in CTLf and OSEF, for all ensemble members. Red dot in Figure 4h shows maximum value point of difference in ensemble spread of Z300 between CTLf and OSEF (MVPΔZ300). Red and blue triangles in Figures 4i-k indicate centers of surface cyclones and anticyclones in CTL, CTLf, and OSEF, respectively.

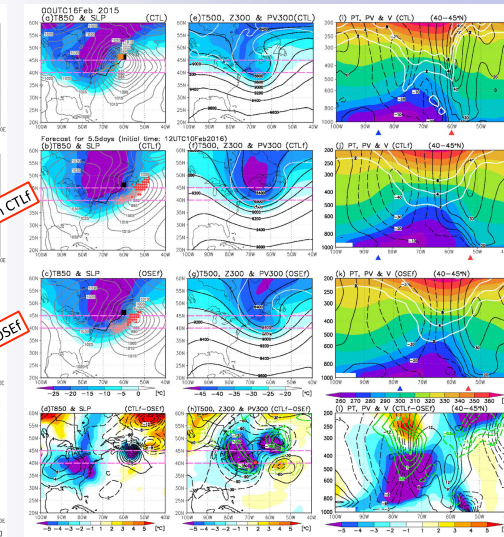


Figure 5: Same as Figure 4 but for North America at 0000 UTC 16 February 2015.

Figure 4: 1850 (color shading: °C) and SLP (contours: hPa) at 0000 UTC 9 February 2015 in (a) CTL, (b) CTLf, and (c) OSEF. Difference between CTLf and OSEF is shown in Figure 4d. (e-f) Same as Figures 4a-d, but for 1500 (color shading: °C), Z300 (contours), and PV at 300 hPa (white lines: 4 PVU). Longitude-height cross sections of PV (color shading: K), meridional winds (black contours: m s<sup>-1</sup>), and PV (white contours: PVU) averaged over areas between 40°N and 45°N (pink lines) shown in Figures 4i-k; the difference between (j) and (k) is also shown in Figure 4l. Black and orange lines in Figure 4a show track of a cyclone from 1800 UTC 7 February through 0000 UTC 9 February in CTL and ERA-Interim. Red lines in Figures 4b and 4c show track of a cyclone from 1800 UTC 7 February through 0000 UTC 9 February in CTLf and OSEF, for all ensemble members. Red dot in Figure 4h shows maximum value point of difference in ensemble spread of Z300 between CTLf and OSEF (MVPΔZ300). Red and blue triangles in Figures 4i-k indicate centers of surface cyclones and anticyclones in CTL, CTLf, and OSEF, respectively.

Figure 5: Same as Figure 4 but for North America at 0000 UTC 16 February 2015.

- 5. Predictive skills and the role of high PV
- Higher skill and smaller uncertainty in Asian case (CTLf) (Fig. 6a)
- Smaller uncertainty in US case (CTLf) (Fig. 6b)
- Difference in ensemble spread of Z300 (MVPΔZ300) was amplified (Fig. 6c)
- MVPΔZ300 traveled with high PV intrusion (Fig. 7e, f)

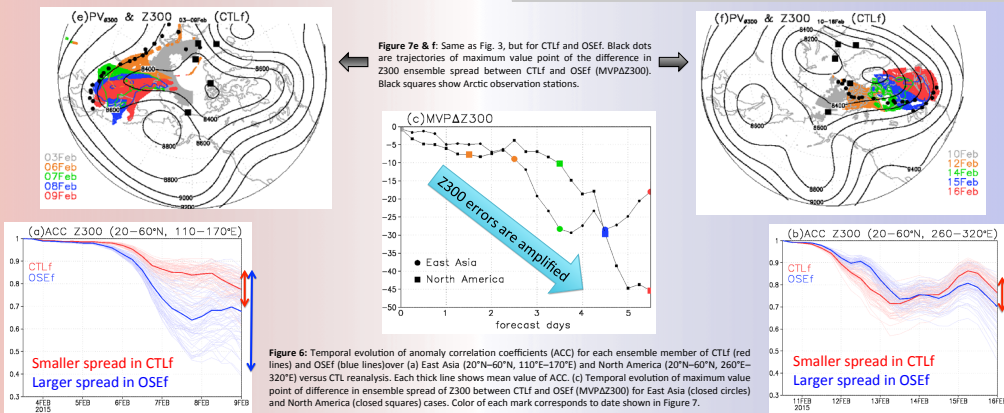


Figure 6: Temporal evolution of anomaly correlation coefficients (ACC) for each ensemble member of CTLf (red lines) and OSEf (blue lines) over (a) East Asia (20°N-60°N, 110°E-170°E) and North America (20°N-60°N, 260°E-320°E) versus CTL reanalysis. Each thick line shows mean value of ACC. (c) Temporal evolution of maximum value point of difference in ensemble spread of Z300 between CTLf and OSEf (MVPΔZ300) for East Asia (closed circles) and North America (closed squares) cases. Color of each mark corresponds to date shown in Figure 7.

## 6. Summary

The observations reduced errors in initial conditions in the upper troposphere over the Arctic region, yielding more precise prediction of the locations and strengths of upper troughs and surface synoptic disturbances. Errors and uncertainties of predicted upper troughs at midlatitudes would be brought with upper level high potential vorticity (PV) intruding southward from the observed Arctic region. This is because the PV contained a "signal" of the additional Arctic observations as it moved along an isentropic surface. This suggests that a coordinated sustainable Arctic observing network would be effective not only for regional weather services but also for reducing weather risks in locations distant from the Arctic. The year of polar prediction (YOPP) from mid-2017 to mid-2019 would provide a great opportunity to explore the roles of polar regions on the predictability of weather extremes at midlatitudes.

**Acknowledgments:** This work was supported by the Arctic Challenge for Sustainability (ARC5) project and KOPRI research project-ICE2015. Simulations were performed on the Earth Simulator with the support of JAMSTEC.

**Reference:** Sato, K., J. Inoue, A. Yamazaki, J.-H. Kim, M. Maturilli, K. Dethloff, S. R. Hudson, and M. A. Granskog (2017), Improved forecasts of winter weather extremes over midlatitudes with extra Arctic observations, *JGR-O*, **122** (in press).